

# FREQUENCY MODULATION EFFECTS IN THE PHOTOINJECTOR FOR THE FERMI@ELETTRA FEL

M. Trovò\*, G. Penco, M. Danailov, Sincrotrone Trieste, Trieste, Italy  
S. Lidia, LBNL, Berkeley, California

## Abstract

In the framework of the FERMI@Elettra project [1], aimed at building a cascaded harmonic FEL x-ray source, a crucial role is played by the electron source, which has to produce a very high quality beam, in terms of low transverse emittance and low uncorrelated energy spread. We have investigated the effects of low (100-300  $\mu\text{m}$ ) and high (10-50  $\mu\text{m}$ ) frequency modulation of the beam current, derived from an intensity modulation of the laser pulse incident on the photocathode, on the downstream longitudinal beam distribution. We present results from simulation of the beam generation at the photocathode, and transport through the photoinjector and initial acceleration modules.

## INTRODUCTION

The temporal profile of the incident ultraviolet laser pulse, that produces electrons from the photocathode, plays a crucial rule in the production of high brightness electron beams from a photoinjector rf gun [2, 3]. The goal in the shaping process is normally to obtain a longitudinal profile that minimizes the normalized transverse emittance and lowers the uncorrelated energy spread of electron bunch which is boosted along the linac accelerator up to the radiator system.

In a soft X-ray FEL source, such as FERMI@Elettra, the seeded laser operation calls for strict tolerances on the acceptable beam quality of the electron beam arriving at the entrance of the undulator system, therefore not only a good electron source is needed but also any beam quality degradation along the machine has to be minimized [4, 5]. The electrons traveling through the acceleration sections and the chicane compressors are subjected to various impedance sources, as those associated with space charge, coherent synchrotron radiation and wakefields. These effects can act as an amplifier on initial electron density and energy modulations, degrading the slice bunch properties.

The profile shaping of a UV laser pulse can lead a temporal modulation in the light pulse, which can be transferred to the longitudinal charge distribution in the bunch. In this paper we present simulations performed with ASTRA and GPT codes [6, 7] with the aim to investigate the behavior of a 1.6 Cell RF gun in the presence of a coherent charge modulation in the electron bunch emitted from the gun's photocathode.

\* mauro.trovo@elettra.trieste.it

## LASER PULSE PROFILE

The desired temporal profile for the UV laser pulse for a photoinjector is the so called 'flat top' shape. Different optical manipulation techniques, like 4-f system [8] or acousto-optic phase modulation (e.g. *DAZZLER*), can be implemented for the longitudinal shaping, though not one of them can avoid some residual profile distortion from the ideal one. The experiments performed so far are encouraging [9, 10] however there seems always to be a residual modulation and its effects have to be considered in studies of electron beam dynamics in photoinjector systems [11].

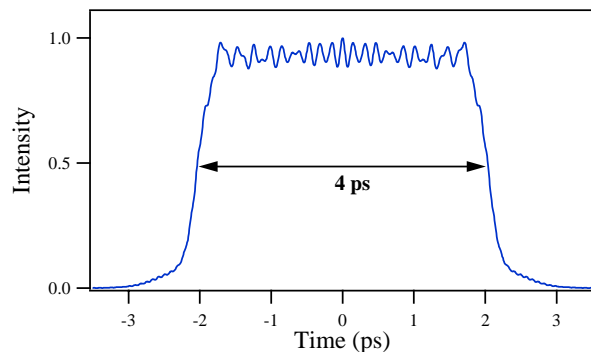


Figure 1: A simulated temporal pulse profile with a desired 4 ps FWHM.

Figure 1 shows a simulated UV laser temporal profile after shaping. We have assumed a pure phase modulation in the frequency domain, which has been chosen by purpose to produce a pulse having features similar to the experimentally observed ones, rather than a perfect flat-top. In particular, we note the non negligible rise/fall times and the high-frequency ripple on the top. The latter was induced by truncating the phase function in the wings of the spectrum, which is one of the realistic causes of noise in 4-f system based shaping technique.

## CHARGE MODULATION

To understand the electron beam dynamics of a modulated bunch in a photoinjector systems, we have started introducing a coherent modulation in the temporal distribution of the emitted electron from the photocathode. The modulation is superposed to the charge distribution used for the short-bunch case at FERMI@Elettra [12].

Figure 2 shows an example of electron distribution that is

tracked in the ASTRA and GPT simulations. In this case, the period of modulation is  $100 \mu\text{m}$  (3 THz) and the relative amplitude is 20%.

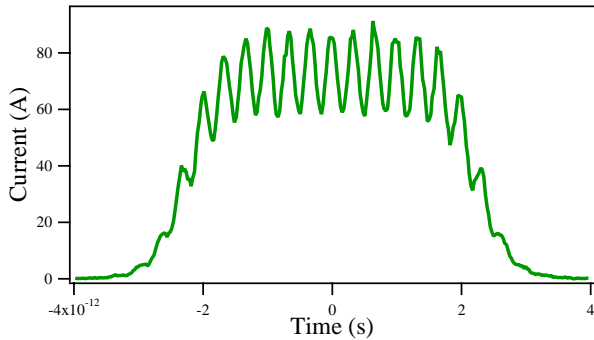


Figure 2: Electron distribution at the cathode emission with a  $100 \mu\text{m}$  modulation period and 20% modulation amplitude.

### Gun filtering

The first simulations were performed by changing the modulation period, sampling the so-called low- and high-frequency range,  $100\text{-}300 \mu\text{m}$  and  $10\text{-}80 \mu\text{m}$  respectively. A dampening of the modulation amplitude was observed in the first few centimeters of the RF cavity, with the gun exhibiting characteristics similar to a low band pass filter. Figure 3 shows the attenuation of longitudinal charge modulation in the low energy beam at the exit of Gun.

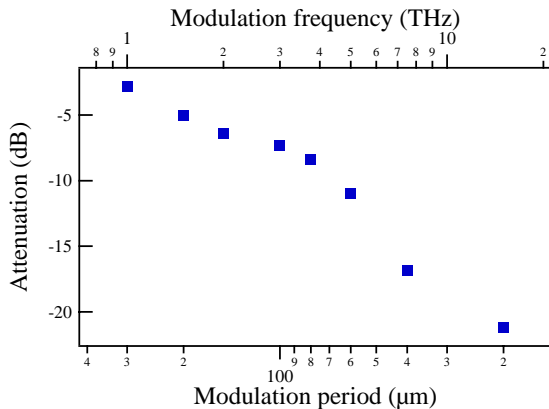


Figure 3: Attenuation in the gun as function of the modulation period with 20% initial amplitude.

In these simulations we start with 20% amplitude at the cathode in order to have a clear signal traceable in its evolution along the system.

### Response

Varying the amplitude of the modulation, we study the case at  $100 \mu\text{m}$  period and we observed an almost linear behavior. In the range of 5-30% of initial amplitude the

damping factor seems to be nearly linear with amplitude (see Figure 4).

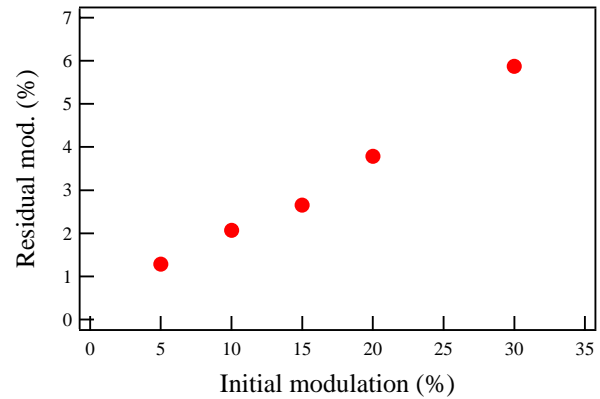


Figure 4: Attenuation in the gun as a function of the modulation amplitude at  $100 \mu\text{m}$ .

### Plasma oscillations

By performing the simulations up to the entrance of first acceleration module we take into account the  $\sim 1.5 \text{ m}$  drift needed for the diagnostics and for the emittance compensation. In this space the 5 MeV beam executes transverse and longitudinal plasma oscillations [13].

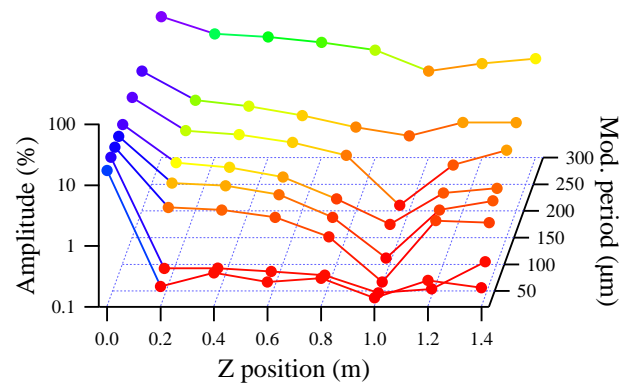


Figure 5: Longitudinal plasma oscillations along the system.

Figure 5 collects data of charge modulation amplitude along the system for various simulations with different modulation periods. Each point is calculated as ratio between the peak value at modulation frequency of the longitudinal charge spectrum and the zero-frequency (DC) component value in the spectrum. After approximately one meter of propagation the bunch reaches a minimum of charge modulation and then begins to rebound, indicating a coherent oscillation. In all simulations the initial modulation is 20% but then the amplitude evolves depending from the period length of modulation. We have also observed a small

coherent shift toward lower frequencies as the beam propagates, presumably resulting from the increasing bunch length.

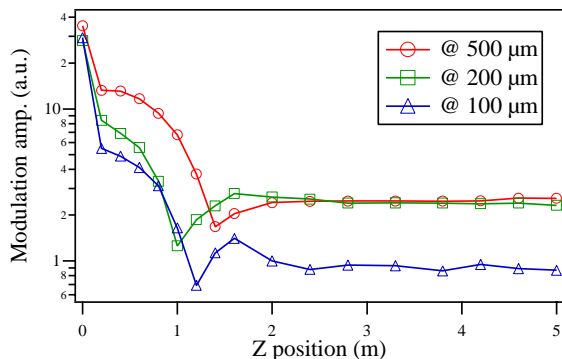


Figure 6: Charge distribution evolution along the system up to the first booster (S0A) exit.

Propagating furthermore the beam, the electrons travel through the first acceleration module (a traveling wave structure denoted as S0A [12]) where they gain  $\sim 50$  MeV energy. Figure 6 shows the simulation results for several modulation periods; in these cases the bunch is rapidly frozen due to the energy gain that reduces the relative spread of longitudinal particle velocities. This effectively halts the longitudinal space charge oscillations at the phase at which the bunch enters the booster linac modules, preserving any remnant charge modulation. The amplitude of residual modulation may be decreased, in a manner similar to transverse space charge emittance compensation, by tailoring the system such that the beam is admitted to the booster linac at the longitudinal oscillation phase which corresponds to a minima in the modulation amplitude.

## ENERGY MODULATION

Considered as a coherent plasma oscillation, charge modulation is transferred into a correlated energy modulation and back. To look at this effect in the previous simulations, we analyze the slice energy distribution along the bunch at different drift positions. After removal of the RF-induced energy correlation from each particle distribution, the slice energy is recorded in a longitudinal bunch energy profile. The slice width is chosen in order to have at least five slices per modulation period. By performing a Fourier transformation we extract the amplitude at the modulation frequency.

Figure 7 shows the evolution of the beam energy modulation along the system. It starts from zero and grows depending on the modulation period. Longer modulation periods lead to deeper energy modulations and the maximum is reached in correspondence with the minimum of the charge modulation. In this analysis, the data presented in Figure 3 is made clearer. The smallest wavelength modulations are quickly damped as they provide no significant correlated velocity spread above the background level gen-

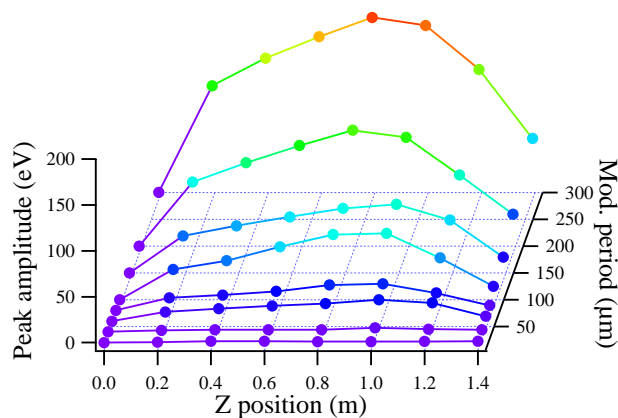


Figure 7: Energy oscillation amplitudes along the system.

erated by DC space charge forces. The medium wavelength modulations (approximately  $50 \mu\text{m} - 100 \mu\text{m}$ ) suffer initial damping at low beam energies but retain sufficient amplitude to initiate a plasma oscillation. Larger wavelength ( $> 100 \mu\text{m}$ ) modulations are the least damped and generate the largest amplitude oscillations.

This kind of analysis is efficient in showing the presence of longitudinal modulation but it is not able to describe completely the phenomena, because it is not sensitive to other microstructures present in the electron distribution. Figure 8 shows the longitudinal phase space of a bunch started at the cathode with a modulation (fig. 8(a)  $80 \mu\text{m}$  and fig. 8(b)  $200 \mu\text{m}$  period), accelerated by the RF gun and propagated through a drift.

By projecting the particles in one dimension to calculate the energy spectrum, the beam filamentation information is lost. Thus the longitudinal energy modulation deep is not sufficient to evaluate the beam sensitivity to the microbunching instability growth in its traveling along the machine.

## CONCLUSION

Coherent modulation of the beam charge has been studied in FERMI@Elettra photoinjector system. The dynamics associated with the longitudinal plasma oscillations have been found to be nearly linear over modulation period range of  $10 \mu\text{m}$  to  $500 \mu\text{m}$ , with modulation amplitude depths of 5-30%. In this region, initial modulations with wavelength smaller than  $\sim 40 \mu\text{m}$  are damped with at least 20 dB of attenuation. Longer wavelength modulations display coherent plasma oscillation with subsequent increase in the modulation amplitude of the slice energy and energy spread. However, previous studies and ongoing work indicate that the wavelengths most likely to undergo gain and instability growth are those that are initially damped the greatest amount. Longer wavelength modulations can be controlled and minimized by careful shaping of the incident laser pulse intensity profile, and possibly by similar techniques as those employed in transverse space charge emittance compensation.

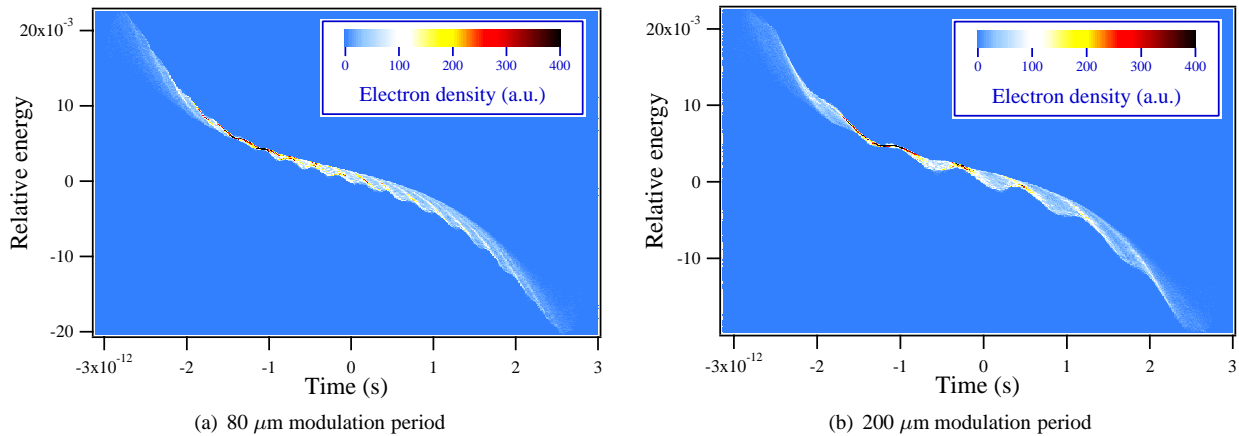


Figure 8: Longitudinal particle phase spaces in the drift (at 80 cm from cathode) started with different modulations.

## REFERENCES

- [1] C. Bocchetta et al., “FERMI @ ELETTRA A seeded harmonic cascade FEL for EUV and soft x-rays”, these proceedings.
- [2] L. Serafini and J. Rosenzweig, “Envelope analysis of intense relativistic quasilaminar beams in rf photoinjectors: a theory of emittance compensation”, *Phys. Rev. E*, **Vol. 55**, 7565 (1997).
- [3] M. Ferrario et al., “New design study and related experimental program for the LCLS RF Photoinjector”, EPAC’00, Vienna, June 2000.
- [4] J. Wu et al., “Temporal profile of the LCLS photocathode ultraviolet drive laser tolerated by the microbunching instability”, LINAC’04, Lübeck, August 2004.
- [5] Z. Huang et al., “Suppression of microbunching instability in the linac coherent light source”, *Phys. Rev. Special Topics*, **Vol. 7**, 074401 (2004).
- [6] K. Flöttman, ASTRA User’s Manual, [https://www.desy.de/~mpyflo/Astra\\_dokumentation](https://www.desy.de/~mpyflo/Astra_dokumentation).
- [7] S.B. Van der Geer et al., “General Particle Tracer Overview”, <http://www.pulsar.nl/gpt/index.html>.
- [8] A. M. Weiner, “Femtosecond pulse shaping using spatial light modulators”, *Review Scientific Instruments*, **Vol. 71**, 1929 (2000).
- [9] H. Loos et al., “Experiments in coherent radiation at SDL”, EPAC’02, Paris, June 2002.
- [10] J. Yang et al., “Experimental studies of photocathode RF gun with laser pulse shaping”, EPAC’02, Paris, June 2002.
- [11] C. Limborg, “UV laser pulse temporal profile requirements for the LCLS injector”, LCLS Technical Note 04-16, Stanford, 2004.
- [12] G. Penco et al., “The RF Injector for the FERMI@Elettra Seeded X-Ray FEL”, these proceedings.
- [13] C. Limborg et al., “Computation of the longitudinal space charge effect in photoinjectors”, EPAC’04, Lucerne, July 2004.